

# The fundamental gas depletion and stellar-mass buildup times of star forming galaxies

Jan Pflamm-Altenburg and Pavel Kroupa

*Argelander-Institut für Astronomie (AIfA), Auf dem Hügel 71, 53121 Bonn, Germany*

`jpflamm@astro.uni-bonn.de, pavel@astro.uni-bonn.de`

## ABSTRACT

Stars do not form continuously distributed over star forming galaxies. They form in star clusters of different masses. This nature of clustered star formation is taken into account in the theory of the integrated galactic stellar initial mass function (IGIMF) in which the galaxy-wide IMF (the IGIMF) is calculated by adding all IMFs of young star clusters. For massive stars the IGIMF is steeper than the universal IMF in star clusters and steepens with decreasing SFR which is called the IGIMF-effect. The current SFR and the total  $H\alpha$  luminosity of galaxies therefore scale non-linearly in the IGIMF theory compared to the classical case in which the galaxy-wide IMF is assumed to be constant and identical to the IMF in star clusters. We here apply for the first time the revised  $SFR-L_{H\alpha}$  relation on a sample of local volume star forming galaxies with measured  $H\alpha$  luminosities. The fundamental results are: i) the SFRs of galaxies scale linearly with the total galaxy neutral gas mass, ii) the gas depletion time scales of dwarf irregular and large disk galaxies are about 3 Gyr implying that dwarf galaxies do not have lower star formation efficiencies than large disk galaxies, and iii) the stellar mass buildup times of dwarf and large galaxies are only in agreement with downsizing in the IGIMF context, but contradict downsizing within the traditional framework that assumes a constant galaxy-wide IMF.

*Subject headings:* cosmology: observations — galaxies: evolution — galaxies: fundamental parameters — stars: formation

## 1. Introduction

The determination of accurate current star formation rates (SFRs) is of fundamental importance for the understanding and investigation of the processes relevant for star formation and galaxy evolution. A commonly used tracer to calculate the current SFR of galaxies is the measurement of the  $H\alpha$  emission line which is linked to the presence of short-lived massive stars.

The standard way to construct relations between the total  $H\alpha$  luminosity and the total SFR of a galaxy is to apply on galaxy-wide scales an invariant stellar initial mass function (IMF) which is determined in star clusters (eg. Kennicutt 1983; Gallagher et al. 1984; Kennicutt et al. 1994; Kennicutt 1998a,b). This method provides a linear  $SFR-L_{H\alpha}$  relation as long as the assumed

galaxy-wide IMF is treated to be constant and independent of the SFR.

A basic result of SFR studies is that  $SFR/M_{\text{gas}}$  decreases with decreasing total neutral gas mass,  $M_{\text{gas}}$ . Low-gas-mass (dwarf irregular) galaxies turn their gas into stars over much longer time scales than high-gas-mass (large disk) galaxies (eg. Skillman et al. 2003; Karachentsev & Kaisin 2007; Kaisin & Karachentsev 2008). That dwarf galaxies have lower star-formation efficiencies, defined as  $\tau_{\text{gas}}^{-1} = SFR/M_{\text{gas}}$ , than massive galaxies has been a generally accepted fact at the base of most theoretical work on galaxy evolution.

But in the last years it has been shown that the application of the IMF in star clusters to galaxy-wide scales is doubtful (Kroupa & Weidner 2003; Weidner & Kroupa 2005, 2006; Hoversten & Glazebrook 2008; Meurer et al. 2009; Lee et al. 2009). In-

stead, the galaxy-wide IMF has to be calculated by adding all IMFs of all young star clusters leading to an integrated galactic stellar initial mass function (IGIMF). The fundamental property of the IGIMF-theory is that for massive stars it steepens with decreasing total SFR although the shape of the underlying IMF in each star cluster is universal and constant. This is a direct consequence of (i) the star formation process taking place in individual embedded star clusters on the scale of a pc, many of which dissolve when emerging from their molecular cloud cores, rather than being uniformly distributed over the galaxy and of (ii) low-star-formation regions being dominated by low-mass star clusters which are void of massive stars (Kroupa & Weidner 2003; Weidner & Kroupa 2005, 2006; Weidner, Kroupa, & Bonnell 2009).

The main aim of this paper is not to present a high precision data analysis of galaxies but to demonstrate the change of fundamental galaxy properties when switching from the constant IMF assumption to the IGIMF theory.

We recap the basics of the IGIMF theory and update its observational support in Section 2. The required data of the sample of star forming galaxies are tabulated in Section 3. We then calculate the SFRs of galaxies (Section 4), gas depletion time scales (Section 5), and stellar mass build-up times (Section 6) using an IGIMF based SFR- $L_{H\alpha}$  conversion and show the dramatic differences that arise from using a constant-IMF based SFR- $L_{H\alpha}$  relation.

## 2. IGIMF: theory and observation

The IMF within each star cluster seems to be universal (Elmegreen 1997, 1999; Kroupa 2001, 2002; Löckmann et al. 2009). The canonical form of the IMF,  $\xi(m) = dN/dm$ , where  $dN$  is the number of stars in the mass interval  $[m, m + dm]$ , is a two-part power law,  $\xi(m) \propto m^{-\alpha_i}$ , in the stellar regime with  $\alpha_1 = 1.3$  for  $0.1 \leq m/M_\odot < 0.5$ ,  $\alpha_2 = 2.35$  for  $0.5 \leq m/M_\odot < m_{\max}$ , where  $m_{\max}$  is the maximal stellar mass in a just-born star cluster with embedded stellar mass  $M_{\text{ecl}}$ . It can also be formulated as a log-normal distribution at low masses and a power-law extension at high masses (Miller & Scalo 1979; Chabrier 2003).

The maximum stellar mass,  $m_{\max}$ , up to which the IMF of a star cluster is populated, is a function

of the total stellar mass,  $M_{\text{ecl}}$ , (Weidner & Kroupa 2006). This relation has been recently confirmed by an updated much larger sample of young embedded star clusters (Weidner et al. 2009).

The masses of young embedded star clusters are distributed according to the embedded cluster mass function (ECMF) (eg. Lada & Lada 2003). The ECMF is populated up to the most massive young star cluster,  $M_{\text{ecl,max}}(\text{SFR})$ . This most massive young star cluster is found to scale with the total SFR of the host galaxy (Weidner, Kroupa, & Larsen 2004).

As stars form in star clusters the galaxy-wide IMF has to be calculated by adding all IMFs of all young star clusters. The embedded star cluster population is dominated by low-mass star clusters and has only a few high-mass star clusters. But due to the  $m_{\max}$ - $M_{\text{ecl}}$  relation massive stars are predominately formed in high-mass clusters, whereas low-mass stars are formed in all star clusters. Thus the resulting integrated galactic stellar initial mass function is steeper than the underlying universal canonical IMF in each star cluster.

With decreasing SFR the upper mass limit of the ECMF decreases and the number ratio of high-mass to low-mass young star clusters decreases. Consequently the galaxy-wide number ratio of high-mass to low-mass young stars decreases, too. As a consequence the IGIMF steepens with decreasing SFR, which we refer to as the IGIMF-effect.

Among all quantities which are relevant for the IGIMF theory the slope of the ECMF is the least accurately constrained one. Thus, two different ECMF-slopes, according to the observational and theoretical range of possible slopes, are used to fully explore the possible range of IGIMF effects: the standard IGIMF with a Salpeter single power-law ECMF slope of  $\beta = 2.35$ , and the minimum-1 IGIMF with a power-law ECMF slope of  $\beta_2 = 2.00$  for star cluster more massive than  $50 M_\odot$  and  $\beta_1 = 1.00$  for star cluster masses between  $5$  and  $50 M_\odot$ . It has been recently suggested that the mass function of young star clusters might be better described by a Schechter-function (Bastian 2008; Larsen 2009). Bastian (2008) obtains a Schechter function with a low mass power-law slope of  $\beta = 2$  below  $M_\star = 1-5 \times 10^6 M_\odot$ . It follows from the SFR-most massive star cluster relation (Weidner et al. 2004) that only galaxies

with  $\text{SFR} \gtrsim 30 M_{\odot} \text{ yr}^{-1}$  populate the ECMF beyond the mass regime described by the power law part of the Schechter function. All galaxies in our sample are below this threshold. Thus the power law description of the ECMF in the IGIMF model includes already a possible global Schechter function of the ECMF for these galaxies.

For a deeper introduction the reader is referred to section 2 of Pflamm-Altenburg et al. (2007) and references therein.

As a consequence, all galaxy-wide properties which depend predominantly on the presence of high-mass stars scale non-linearly with the total SFR, such as the total  $\text{H}\alpha$  luminosity, the oxygen yield, and the alpha-element  $[\alpha/\text{Fe}]$  ratios. The observed mass-metallicity relation of galaxies is a direct outcome of the IGIMF-theory (Köppen et al. 2007) and the decreasing  $[\alpha/\text{Fe}]$  ratio with decreasing velocity dispersion of galaxies can be easily explained in the IGIMF context (Recchi et al. 2009). In both cases no extreme fine-tuning and parameter adjustment is required as is the case if a constant IMF on galaxy scales is assumed.

The IGIMF-theory connects the galaxy-wide IMF with the current SFR and thus refers to whole galaxies. Within galaxies star formation is described by the corresponding surface star formation rate density,  $\Sigma_{\text{SFR}} = dM/dtdxdy$ , which defines the newly formed stellar mass,  $dM$ , per time interval,  $dt$ , and per area,  $dxdy$ . In order to construct a local relation between the local star formation rate surface density,  $\Sigma_{\text{SFR}}$ , and the produced local  $\text{H}\alpha$  luminosity surface density,  $\Sigma_{\text{H}\alpha} = dL_{\text{H}\alpha}/dtdxdy$ , which defines the produced  $\text{H}\alpha$  luminosity,  $dL_{\text{H}\alpha}$ , per time interval,  $dt$ , and per area,  $dxdy$ , the embedded cluster mass function and the integrated galactic stellar initial mass function are replaced in the IGIMF theory by their corresponding surface densities. These are the local embedded cluster mass function, LECMF, and the local integrated galactic stellar initial mass function, LECMF. In the outer regions of disk galaxies the star formation rate surface density is lower and the LECMF is populated to lower upper masses than in the inner regions. Like the IGIMF effect for whole galaxies, a local IGIMF effect emerges. Thus the  $\text{H}\alpha$  luminosity surface density decreases faster with increasing radial distance than the star formation rate surface den-

sty, which naturally explains the radial  $\text{H}\alpha$  cut-off in disk galaxies (Pflamm-Altenburg & Kroupa 2008).

How the  $\text{H}\alpha$  based SFRs of galaxies and their related properties change when the classical linear  $L_{\text{H}\alpha}$ -SFR relation is replaced by the non-linear IGIMF based conversion, presented in Pflamm-Altenburg et al. (2007), is explored in this paper. The classical relation between the total  $\text{H}\alpha$  luminosity of a galaxy and the underlying SFR is based on the assumption that the galaxy-wide IMF is identical to the IMF observed in star clusters and does not vary with SFR. Thus, the classical SFR scales linearly with the total  $\text{H}\alpha$  luminosity. The relation between the total SFR and the total  $\text{H}\alpha$  luminosity in the IGIMF theory is nearly linear in the high  $\text{H}\alpha$  luminosity range, i.e. for  $L_*$  and more luminous galaxies. But the IGIMF-based SFR- $L_{\text{H}\alpha}$  relation deviates increasingly from linearity for  $\text{H}\alpha$  faint galaxies, i.e. for galaxies with an  $\text{H}\alpha$  luminosity comparable to the SMC ( $\approx 5 \times 10^{39} \text{ erg s}^{-1}$ ) or less. Thus, the classical method underestimates the SFR of  $\text{H}\alpha$  faint galaxies compared to the IGIMF prediction. This underestimation is illustrated in Fig. 1. The SFR for both IGIMF models (standard and minimal) are calculated using the fifth-order polynomial fit published in section 2.3 and tab. 2 in Pflamm-Altenburg et al. (2007). The classical SFR is calculated with the widely used linear relation by Kennicutt et al. (1994),

$$\frac{\text{SFR}}{M_{\odot} \text{ yr}^{-1}} = \frac{L_{\text{H}\alpha}}{1.26 \times 10^{41} \text{ erg s}^{-1}} \cdot \quad (1)$$

For example, a galaxy with an  $\text{H}\alpha$  luminosity of  $1.26 \times 10^{38} \text{ erg s}^{-1}$  has a classical Kennicutt-SFR of  $10^{-3} M_{\odot} \text{ yr}^{-1}$ . The IGIMF SFR is 5 times larger for the minimal model and 10 times larger in the standard model.

Additionally the IGIMF-effect is expected to have different strengths for  $\text{H}\alpha$  and FUV radiation, because the  $\text{H}\alpha$  luminosity depends only on the presence of the ionising radiation of short-lived high-mass stars, whereas long-lived B stars also contribute to the FUV flux. It has been predicted that the  $\text{H}\alpha/\text{FUV}$  flux ratio decreases with decreasing SFR (Pflamm-Altenburg et al. 2009). Recently Meurer et al. (2009) have shown that the  $\text{H}\alpha/\text{FUV}$  flux ratio of star forming galaxies decreases with decreasing average  $\text{H}\alpha$  surface lumi-

nosity density and conclude that a varying galaxy-wide IMF slope in dependence of the SFR might be the most likely explanation. A different study by Lee et al. (2009) of local volume galaxies found a decreasing  $H\alpha$ /FUV flux ratio with decreasing total  $H\alpha$  luminosity which is in remarkable quantitative agreement with the prediction by the IGIMF theory by Pflamm-Altenburg et al. (2009) down to the least-massive dwarf galaxies.

A more detailed listing and discussion of the observational support of the IGIMF theory is given in section 1 of Pflamm-Altenburg, Weidner, & Kroupa (2009).

It should be emphasised here that one may argue that anything can be explained by a suitably chosen variable IMF. But how the IGIMF varies is not adjusted for the problem to be solved or explained. Instead, the nature of clustered star formation defines how the slope of the IGIMF scales with the total SFR. This means the slope of the IGIMF is defined by the SFR of the galaxy. The relation between the IGIMF-slope and the current SFR is constant for all applications. There is no freedom to match the galaxy-wide IMF slope for a considered problem. Although the slope of the IGIMF varies the IMF in star clusters is universal and constant and not varying, i.e. the star formation physics is untouched.

### 3. Data

In order to calculate current SFRs, gas depletion times and stellar mass buildup time scales of star forming galaxies in the IGIMF-context, the  $H\alpha$  luminosity,  $L_{H\alpha}$ , the total neutral gas mass,  $M_{\text{gas}}$ , and the blue band absolute magnitude,  $M_B$ , of 200 local volume galaxies (Tab. 1) are compiled from different samples of star forming galaxies: the Canes Venatici I group of galaxies (Kaisin & Karachentsev 2008), the M81 galaxy group (Karachentsev & Kaisin 2007), the dwarf irregular galaxies of the Sculptor group (Skillman et al. 2003), a sample of isolated dwarf irregular galaxies (van Zee 2001), local group dwarf irregular galaxies (Mateo 1998) and the local group disk galaxies, M31, M33 (Walterbos & Braun 1994; Dame et al. 1993; Karachentsev et al. 2004; Verley et al. 2007; Corbelli & Schneider 1997; Kennicutt et al. 1995; Hindman 1967; Westerland 1997). In most cases the  $H\alpha$  luminosity was

not given. Instead, the published SFR, based on the observed  $H\alpha$  luminosity, has been transformed into the  $H\alpha$  luminosity using the respective SFR- $L_{H\alpha}$  relation as described in the publication where the SFR is extracted from. The published SFR, based on a linear SFR- $L_{H\alpha}$  relation (eg. Kennicutt et al. 1994), is tabulated in Table 1 (Col. 5). The observed total  $H\alpha$ -luminosity (Col. 2) is converted into an IGIMF-SFR using the relations given in Pflamm-Altenburg et al. (2007) for the standard-IGIMF model (Col. 6) and the minimal1-IGIMF model (Col. 7) in order to cover the range of IGIMFs allowed by the empirical data (Sec. 2).

The Milky Way is included in this study. The HI mass is taken from van den Bergh (1999). Due to the lack of  $H\alpha$  data for the Milky Way we take the SFR from Diehl et al. (2006) which is based on the measurement of the Al-26 and Fe-60 gamma ray flux. As this SFR determination is based on a Scalo slope of  $\alpha = 2.7$  in the high-mass regime of the IMF, the IGIMF-effect is already taken unknowingly into account.

The total neutral gas mass (Col. 3) is the total HI mass taken from the references multiplied by 1.32, following Skillman et al. (2003), to account for primordial helium. The absolute B-band magnitudes are listed in Col. 4.

Other HI-total-gas-mass conversion factors have been applied in the literature, eg. 1.34 (Kunth & Sargent 1986; Legrand et al. 2001) or 1.36 (Kennicutt et al. 2007). The conversion factor may therefore be uncertain by 3 per cent, corresponding to a logarithmic uncertainty of the total neutral gas mass of  $\Delta \log_{\text{HI}} = 0.013$ . For the purpose of this study this uncertainty can be neglected and we use a factor of 1.32, following Skillman et al. (2003), throughout this study.

Finally it should be noted that the galaxies of our sample stem from different observations. Values from 21 cm and optical observations are compared with each other. As HI exists to much larger galactocentric radii than  $H\alpha$  radiation is produced, the areas covered by the observations are differently large. Because our study compares total integrated values with each other the differently large areas do not impose a problem here. The observed  $H\alpha$  luminosities might suffer from a bias as the different observations might have been performed with differently defined surface bright-

ness limits. Given that the  $H\alpha$  surface brightness strongly declines with increasing galactocentric radius in star forming galaxies, the main contribution to the total  $H\alpha$  luminosity comes from the inner regions of the galaxies which should be covered by each observation. The very small possible bias for the total  $H\alpha$  luminosities can be neglected here, because the main aim of our study is to demonstrate the differences which arise when the classical method for calculating SFRs from total  $H\alpha$  luminosities based on a constant galaxy-wide IMF is replaced by the IGIMF-based conversion resulting in new SFRs being up to a factor 100 larger.

In order to detect possible differences between the different data sources all galaxies which belong to the same sub-sample are plotted by the same symbol. These sub-samples are the Canes Venatici cloud of galaxies (CVnI), the M81 group, the Sculptor group of dwarf irregular galaxies, a sample of isolated dwarf irregular galaxies, the local group of star forming galaxies, and the Milky Way. It can be seen in the following plots that the changes of the SFRs with decreasing galaxy mass are the same for all sub-samples. A systematic bias between the various sub-samples is thus not evident.

Although these sub-samples cover different regions in the local volume, some overlap exists with the sub-sample of *isolated dwarf irregular galaxies* by van Zee (2001). Nine galaxies have been identified to be listed twice in Table 1 (see Table 2). These galaxies appear twice in the following plot as independent data.

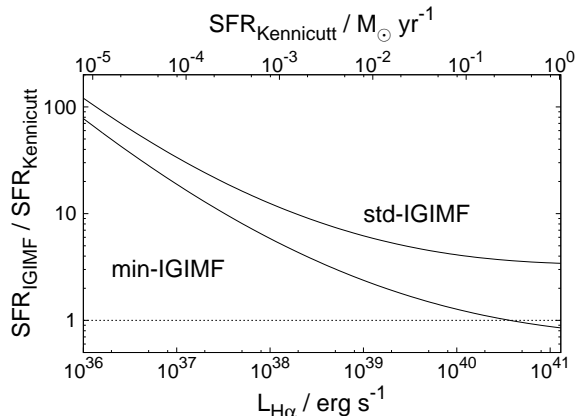


Fig. 1.— Ratio of the SFRs calculated from the observed  $H\alpha$  luminosity with the classical constant-IMF based conversion from Kennicutt et al. (1994) and the IGIMF based conversion from Pflamm-Altenburg et al. (2007). The IGIMF-based SFRs are calculated using the fifth-order polynomial fit published in section 2.3 and tab. 2 in Pflamm-Altenburg et al. (2007).

TABLE 1  
GALAXY PROPERTIES

Galaxy	$\log L_{\text{H}\alpha}$ erg / s	$\log M_{\text{gas}}$ $M_{\odot}$	$M_{\text{B}}$	$\log \text{SFR}$ $M_{\odot} / \text{yr}$ IMF	$\log \text{SFR}$ $M_{\odot} / \text{yr}$ std-IGIMF	$\log \text{SFR}$ $M_{\odot} / \text{yr}$ min-IGIMF	Ref. SFR, $L_{\text{H}\alpha}$	Ref. $M_{\text{HI}}$	Ref. $M_{\text{B}}$
UGC 5427	38.78	7.61	-14.48	-2.19	-1.47	-1.87	(1)	(1)	(1)
UGC 5672	38.87	7.52	-14.65	-2.10	-1.40	-1.81	(1)	(1)	(1)
NGC 3274	39.86	8.86	-16.16	-1.11	-0.60	-1.10	(1)	(1)	(1)
NGC 3344	40.71	9.79	-19.03	-0.26	0.17	-0.41	(1)	(1)	(1)
UGC 6541	39.29	7.15	-13.71	-1.68	-1.08	-1.52	(1)	(1)	(1)
NGC 3738	39.67	8.21	-16.61	-1.30	-0.77	-1.25	(1)	(1)	(1)
NGC 3741	38.69	8.17	-13.13	-2.28	-1.53	-1.92	(1)	(1)	(1)

NOTE.—Table 1 is published in its entirety in the electronic edition of the *Astrophysical Journal*. A portion is shown here for guidance regarding its form and content. References: (1) Kaisin & Karachentsev (2008), (2) Karachentsev & Kaisin (2007), (3) Skillman et al. (2003), (4) Mateo (1998), (5) van Zee (2001), (6) Walterbos & Braun (1994), (7) Dame et al. (1993), (8) Karachentsev et al. (2004), (9) Verley et al. (2007), (10) Corbelli & Schneider (1997), (11) Kennicutt et al. (1995), (12) Hindman (1967), (13) Westerlund (1997), (14) Diehl et al. (2006), (15) van den Bergh (1999).

TABLE 2  
MULTIPLY LISTED GALAXIES

Galaxy (ref.)	Galaxy (ref.)
UGCA 292 (1)	UGCA 292 (5)
DDO 181 (1)	UGC 8651 (5)
DDO 183 (1)	UGC 8760 (5)
UGC 8833 (1)	UGC 8833 (5)
DDO 187 (1)	UGC 9128 (5)
DDO 190 (1)	UGC 9240 (5)
UGC 5423 (2)	UGC 5423 (5)
DDO 226 (3)	UGCA 9 (5)
DDO 6 (3)	UGCA 15 (5)

NOTE.—Each line refers to one galaxy which is listed in different references. The references are the same as in Table 1. For example, the second line shows that the same galaxy is listed as DDO 181 in reference (1) and as UGC 8651 in reference (5).

#### 4. Calculating SFRs

The SFRs, which are taken from the literature and based on a classical linear conversion of the H $\alpha$  luminosity into a SFR (eg. Kennicutt et al. 1994), are plotted in dependence of the total galaxy neutral gas mass in Fig. 2. With decreasing galaxy neutral gas mass the relation between the traditionally calculated SFR and the galaxy neutral gas mass becomes increasingly steeper. Here we find that for massive galaxies of our sample with neutral gas masses  $\geq 5 \times 10^7 M_\odot$  the SFR scales slightly non-linear with neutral gas mass,

$$\frac{SFR}{M_\odot \text{ yr}^{-1}} = 3.91 \times 10^{-13} \left( \frac{M_{\text{gas}}}{M_\odot} \right)^{1.26}, \quad (2)$$

and scales almost quadratically for less massive galaxies ( $M_{\text{gas}} \leq 5 \times 10^7 M_\odot$ ),

$$\frac{SFR}{M_\odot \text{ yr}^{-1}} = 7.96 \times 10^{-18} \left( \frac{M_{\text{gas}}}{M_\odot} \right)^{1.87}. \quad (3)$$

This behaviour is already well known (e.g. Karachentsev & Kaisin 2007; Kaisin & Karachentsev 2008).

The non-linear relation between the total H $\alpha$  luminosity and the underlying SFR calculated with the IGIMF-theory diverges significantly from these classical linear relations based on a constant galaxy-wide IMF below SFRs typical for SMC-type galaxies. For comparison, the SFR- $M_{\text{gas}}$  relation in the classical picture becomes increasingly steeper for galaxy masses less than SMC-type galaxies. It can be expected that the IGIMF theory revises the H $\alpha$ -SFRs of galaxies with a small neutral gas content such that their lower star formation efficiencies will be increased. The SFR- $M_{\text{gas}}$  relation of this galaxy sample as resulting from the IGIMF theory is shown in Fig. 3 for the standard model and in Fig. 4 for the minimum model.

It can be clearly seen that for both IGIMF models the turn-down evident in the classical SFR- $M_{\text{gas}}$  relation (Fig. 2) disappears completely.

For the standard IGIMF a bivariate regression gives a linear scaling of the total SFR and the galaxy neutral gas mass,

$$\frac{SFR}{M_\odot \text{ yr}^{-1}} = 3.97 \times 10^{-10} \left( \frac{M_{\text{gas}}}{M_\odot} \right)^{0.99}. \quad (4)$$

For the minimum IGIMF the relation between the SFR and the galaxy neutral gas mass is

$$\frac{SFR}{M_\odot \text{ yr}^{-1}} = 1.62 \times 10^{-9} \left( \frac{M_{\text{gas}}}{M_\odot} \right)^{0.87}. \quad (5)$$

Note that the main parameter in the IGIMF theory is the slope of the ECMF. Both IGIMF models, the standard model with an ECMF slope of  $\beta = 2.35$  and the minimum model with an ECMF slope of  $\beta = 2$ , cover the full range of possible ECMFs. Therefore, the change that emerges in the SFR- $M_{\text{gas}}$  relation when changing from the classical invariant IMF description to the IGIMF theory is a direct result of the nature of clustered star formation.

In conclusion, the IGIMF theory revises the SFRs of dwarf galaxies significantly, such that the true SFRs may be larger than hitherto thought by two or three orders of magnitude. The reason why this was not evident until now comes about because in dwarf galaxies star formation predominantly occurs in low-mass clusters which do not contain massive stars.

#### 5. Gas depletion time scales

The gas depletion time scale,  $\tau_{\text{gas}}$ , is a measure for how long a galaxy with current total neutral gas mass,  $M_{\text{gas}}$ , can sustain its current SFR without being refueled by accretion of fresh extragalactic material. It is defined by

$$\tau_{\text{gas}} = \frac{M_{\text{gas}}}{SFR}. \quad (6)$$

The corresponding gas depletion time scales, based on a constant galaxy-wide IMF, are plotted in Fig. 5.

The SFR- $M_{\text{gas}}$  relations for the IMF case (eq. 2 and 3) can now be converted into  $\tau_{\text{gas}}$ -SFR relations, which are plotted as dashed lines in Fig. 5. The gas depletion time scale increases slightly with decreasing total galaxy neutral gas mass for galaxies more massive than  $5 \times 10^7 M_\odot$  and it increases strongly for less-massive galaxies with masses less than  $5 \times 10^7 M_\odot$ , in agreement with other studies (Skillman, Côté, & Miller 2003; Bothwell, Kennicutt, & Lee 2009). This is commonly interpreted as star forming dwarf galaxies having much lower star formation efficiencies,  $\tau_{\text{gas}}^{-1}$ , than large disk galaxies.



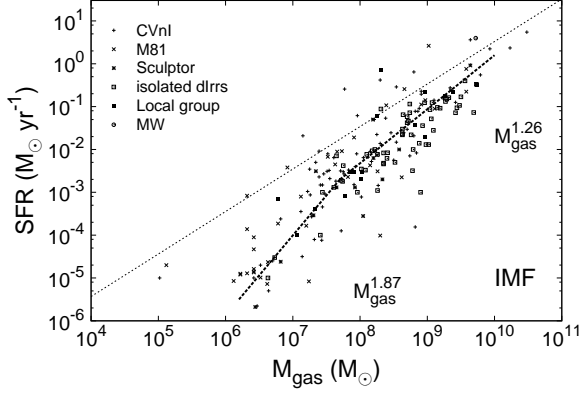


Fig. 2.— The original SFRs taken from the literature are plotted versus the host galaxy total neutral gas mass. These SFRs are calculated from the total  $H\alpha$  luminosity using a classical linear SFR- $L_{H\alpha}$  relation. Galaxies with a total neutral gas mass  $\gtrsim 10^8 M_\odot$  show a  $SFR \propto M_{\text{gas}}^{1.26}$  relation (eq. 2), whereas the SFRs of less massive galaxies scale with  $M_{\text{gas}}^{1.87}$  (eq. 3), both bivariate fits being shown as thick-dotted lines. For comparison, the thin dotted line shows the bivariate regression from Fig. 3 of the standard IGIMF model with slope 0.99.

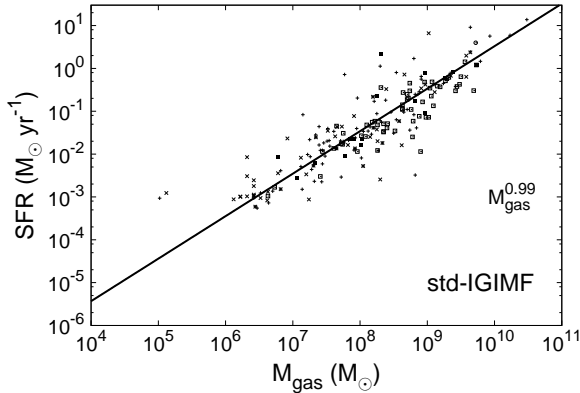


Fig. 3.— The calculated SFRs based on the standard IGIMF versus the total galaxy neutral gas mass. The solid line shows the bivariate regression for the standard IGIMF (eq. 4). The symbols are the same as in Fig. 2.

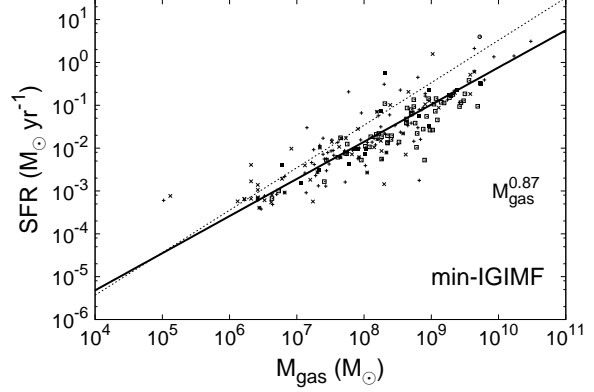


Fig. 4.— Same as Fig. 3 but using the SFR- $L_{H\alpha}$  relation based on the minimum-IGIMF. The solid line shows the bivariate regression for this minimum IGIMF (eq. 5). For comparison, the dotted line shows the fit of the standard model (eq. 4). The symbols are the same as in Fig. 2.

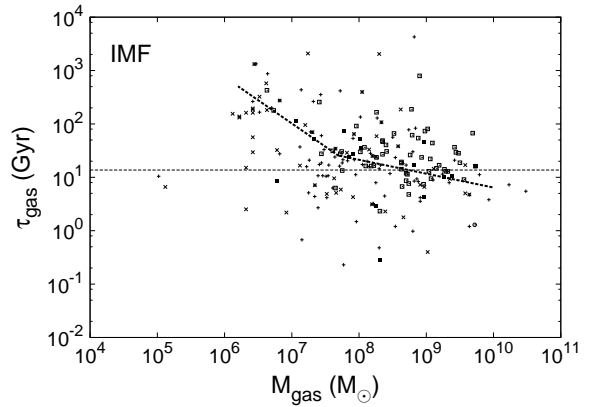


Fig. 5.— Gas depletion time scales in dependence of the total galaxy neutral gas mass for the case of a constant galaxy-wide IMF. The thin dotted line marks the age of the universe, 13.7 Gyr. The symbols are the same as in Fig. 2.

In the previous section it has been shown that the SFRs of dwarf galaxies are much higher if the constant galaxy-wide IMF is replaced by the IGIMF, and consequently the gas depletion time scales are now expected to be shorter.

The resulting gas depletion time scales for the standard IGIMF are plotted in Fig. 6 and for the minimum IGIMF in Fig. 7. In both cases the gas depletion time scales of dwarf galaxies are comparable to the gas depletion time scales of large disk galaxies.

For the standard IGIMF the SFR scales linearly with the total galaxy neutral gas mass (eq. 4). The resulting gas depletion time scale with the total galaxy neutral gas mass as

$$\tau_{\text{gas}} = \frac{M_{\text{gas}}}{\text{SFR}} = 2.52 \text{ Gyr} \left( \frac{M_{\text{gas}}}{M_{\odot}} \right)^{0.01}. \quad (7)$$

The mean gas depletion time scale of a galaxy with a neutral gas mass of  $10^6 M_{\odot}$  is 2.89 Gyr and for a galaxy with a neutral gas mass of  $10^{10} M_{\odot}$  it is 3.17 Gyr. Thus, the gas depletion time scales are constant for all galaxies, being approximately 3 Gyr. It follows that low-mass dwarf irregular galaxies have the same star formation efficiency as massive disk galaxies, in disagreement with the currently widely accepted notion according to which dwarf galaxies are inefficient in making stars.

The gas depletion time scales for the standard IGIMF are not only shorter than the IMF gas depletion time scales, but they also have a smaller scatter. Fig. 8 shows the normalised histogram of the gas depletion time scales for the IMF case (dashed histogram) and for the standard IGIMF case (solid histogram). The scatter of the standard IGIMF gas depletion time scales can be well described by a log-normal distribution,

$$\frac{dN_{\text{Gal}}}{d \log \tau_{\text{gas}}} = \frac{1}{\sqrt{2\pi\sigma^2}} e^{-\frac{(\log \tau_{\text{gas}} - \mu)^2}{2\sigma^2}}, \quad (8)$$

with  $\mu = 9.50$  (3.19 Gyr),  $\sigma = 0.36$ . If and to what degree conclusions can be made for the physical conditions for star formation on the basis of the reduced scatter in the IGIMF gas depletion time scales is unclear at the moment. A volume limited sample in further studies is required in order to avoid any kind of bias.

In the case of the minimum IGIMF the resultant  $\tau_{\text{gas}}-M_{\text{gas}}$  relation follows from eq. 5,

$$\tau_{\text{gas}} = \frac{M_{\text{gas}}}{\text{SFR}} = 0.62 \text{ Gyr} \left( \frac{M_{\text{gas}}}{M_{\odot}} \right)^{0.13}. \quad (9)$$

This leads to a gas-depletion time scale of 3.74 Gyr for a  $10^6 M_{\odot}$  galaxy and 12.37 Gyr for a  $10^{10} M_{\odot}$  galaxy. This means that in the case of the minimum IGIMF dwarf irregular galaxies consume their gas faster than large disk galaxies and would therefore have higher star-formation efficiencies in contradiction to the currently widely accepted picture.

Thus, independent of the IGIMF model details dwarf galaxies do not have lower star formation efficiencies than large disk galaxies.

## 6. Blue stellar mass buildup times

In the previous section the current SFR and available total neutral gas mass of galaxies have been analysed to calculate their current gas depletion time scales. This allows an estimation of their future star formation activity. Here we now compare the current SFR, and the already assembled total stellar mass,  $M_*$ , of galaxies to analyse their past star formation by calculating the corresponding stellar mass buildup time scale,  $\tau_*$ , which is defined by

$$\tau_* = \frac{M_*}{\text{SFR}}. \quad (10)$$

The total stellar mass is here calculated from the blue-band magnitude,  $M_B$ , (Tab. 1, Col. 4). In order to account for possible different metallicities and star formation histories (SFHs), we use the stellar-mass-to-light-ratio-colour relations published by Bell & de Jong (2001). These relations are obtained from synthetic spectra based on different galaxy evolution models with a constant galaxy-wide IMF. Bell & de Jong (2001) adopt a large variety of star formation histories as indicated in Tab. 3.

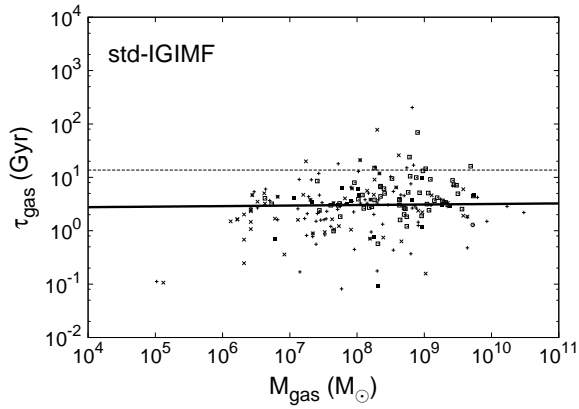


Fig. 6.— Same as Fig. 5 but for the case of the standard IGIMF. The solid line shows eq. 7, while the thin dotted line marks the age of the universe as in Fig. 5. Note the reduced scatter in comparison to Fig. 5. The symbols are the same as in Fig. 2.

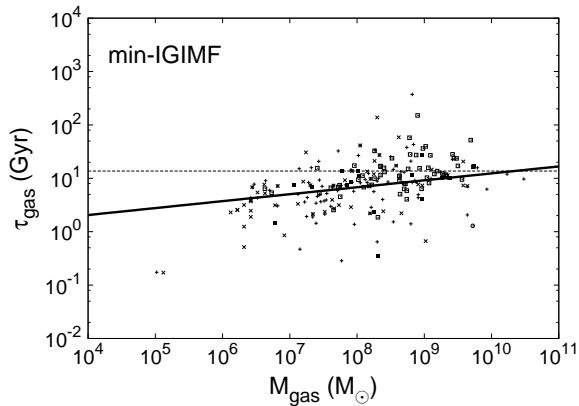


Fig. 7.— Same as Fig. 5 but for the case of the minimum IGIMF. The solid line shows eq. 9. The symbols are the same as in Fig. 2.

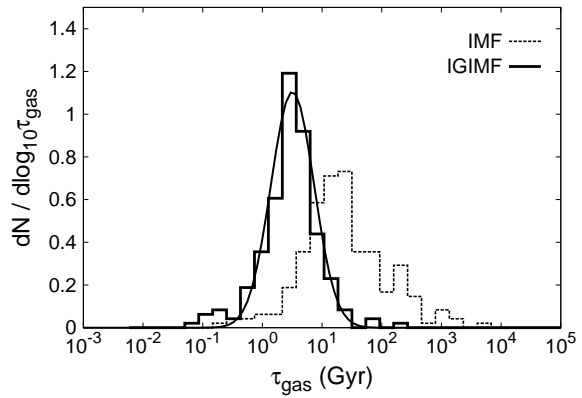


Fig. 8.— The normalised histogram of gas depletion time scales for the constant IMF (Fig. 5) and the standard IGIMF (Fig. 6) overlaid with the log-normal distribution of eq. 8. Note that the IGIMF-based gas depletion time scales are significantly shorter on average, have a symmetric distribution, and have a significantly smaller dispersion than if the galaxy-wide IMF is assumed to be invariant.

TABLE 3  
 STELLAR-MASS-TO-LIGHT-RATIO-COLOUR RELATIONS

Model	$a_{\text{B,B-H}}$	$b_{\text{B,B-H}}$
Closed Box	-1.551	0.586
Infall	-1.706	0.621
Outflow	-1.466	0.555
Dynamical time	-1.505	0.564
Formation epoch	-1.741	0.630
Formation epoch burst	-1.764	0.634
Cole et al. 2000	-1.699	0.621
Mean	-1.633	0.602

NOTE.—The coefficients  $a_{\text{B,B-H}}$  (eq. 14) and  $b_{\text{B,B-H}}$  (eq. 15) have been derived from different galaxy evolution models (Bell & de Jong 2001) and the corresponding mean values.

It might be argued that the application of these relations is wrong because the IGIMF will affect the stellar-mass-to-light-ratio-colour relations. In Pflamm-Altenburg et al. (2009) it has been shown that for small SFRs the IGIMF effect for the FUV-flux is less than one dex if the IGIMF effect for H $\alpha$  is two dex. The B-band and longer wavelength bands are expected to show an even smaller IGIMF effect than the FUV-flux. The dominating influence on the stellar mass buildup time scale is by far the IGIMF-effect for the H $\alpha$  based SFRs (eq. 10). Thus, the Bell & de Jong (2001) stellar-mass-to-light-ratio-colour relations are applicable for an order-of-magnitude estimate of the stellar mass buildup times. However, precision galaxy evolution modeling would require revised mass-to-light ratios, which we will address in future projects.

The two stellar-mass-to-light-ratio-colour relations

$$\log \frac{M_*}{L_B} = a_{B,B-V} + b_{B,B-V} (M_B - M_V) , \quad (11)$$

and

$$\log \frac{M_*}{L_B} = a_{B,V-H} + b_{B,V-H} (M_V - M_H) , \quad (12)$$

tabulated in Bell & de Jong (2001) can be used to construct a stellar-mass-to-light-ratio-colour relation between the B-band magnitude and the B-H colour,

$$\log \frac{M_*}{L_B} = a_{B,B-H} + b_{B,B-H} (M_B - M_H) , \quad (13)$$

where the two coefficients are given by

$$a_{B,B-H} = \frac{b_{B,V-H} a_{B,B-V} + b_{B,B-V} a_{B,V-H}}{b_{B,V-H} + b_{B,B-V}} , \quad (14)$$

and

$$b_{B,B-H} = \frac{b_{B,V-H} b_{B,B-V}}{b_{B,V-H} + b_{B,B-V}} , \quad (15)$$

The required colour is obtained using the tabulated blue-band magnitude, and the H-band magnitude,  $M_H$ . To assign an H-band magnitude to each galaxy we use the observed extremely tight correlation between the B- and H-band magnitude of galaxies (Kirby et al. 2008, eq. 9) ranging from  $M_B = -8$  to  $M_B = -22$ . The resulting empirical relation between the B-H colour and the B-band is then given by

$$M_B - M_H = -0.14 M_B + 0.74 . \quad (16)$$

In Bell & de Jong (2001) the stellar-mass-to-light-ratio-colour relations are given for seven different galaxy evolution models, which lead to slightly different values for  $a_{B,B-V}$ ,  $a_{B,V-H}$ ,  $b_{B,B-V}$ , and  $b_{B,V-H}$ . The resulting coefficients,  $a_{B,B-H}$  and  $b_{B,B-H}$ , are listed in Tab. 3. In the following analysis we use their mean values for the  $\log M_*/L_B - (M_B - M_H)$  relation,

$$a_{B,B-H} = -1.633 \quad \text{and} \quad b_{B,B-H} = 0.602 . \quad (17)$$

We now have for each of our galaxies  $M_B$  (Tab. 1, Col 4),  $M_H$  (from eq. 16) and thus  $M_*/L_B$  (from eq. 13). Each of the  $M_B$  values can therefore be converted to the total stellar mass  $M_*$  allowing the computation of  $\tau_*$  for each galaxy.

For a few galaxies of our sample absolute H-band magnitudes are listed in Kirby et al. (2008). For these galaxies we use the observed absolute H-band magnitude, for all the others we use the calculated B-H colour according to the procedure described above. Table 4 lists those galaxies which have observed absolute H-band magnitudes by Kirby et al. (2008).

TABLE 4  
OBSERVED VS. CALCULATED H-BAND MAGNITUDES

Galaxy	$M_{\text{H,obs.}}$	$M_{\text{B,obs.}} - M_{\text{H,obs.}}$	$M_{\text{B,obs.}} - M_{\text{H,cal.}}$	$\log M_{*,\text{obs.}}$ $M_{\odot}$	$\log M_{*,\text{cal.}}$ $M_{\odot}$	$M_{*,\text{obs.}}/M_{*,\text{cal.}}$
SC 18	-11.5	2.30	2.03	5.62	5.46	1.45795
ESO 473-G24	-16.1	3.42	2.52	7.69	7.15	3.50501
SC 24	-10.7	2.31	1.91	5.31	5.07	1.72994
NGC 625	-19.2	2.89	3.02	8.82	8.90	0.831176
ESO 245-G05	-17.2	1.61	2.92	7.76	8.55	0.162112
DDO 210	-12.9	1.94	2.27	6.11	6.31	0.629059
ESO 347-G17	-18.3	3.51	2.81	8.59	8.17	2.63657
ESO 348-G09	-17.2	3.45	2.67	8.14	7.66	2.96873

NOTE.—Listed are those galaxies of Table 1 for which absolute H-band magnitudes,  $M_{\text{H,obs.}}$ , are published in Kirby et al. (2008). Two B-H colors and two total stellar masses based on eq 13 and 17 are calculated:  $M_{\text{B,obs.}} - M_{\text{H,obs.}}$  and  $\log M_{*,\text{obs.}}$  are based on the observed absolute B-band (Table 1) and the observed absolute H-band magnitude (Kirby et al. 2008).  $M_{\text{B,obs.}} - M_{\text{H,cal.}}$  and  $\log M_{*,\text{cal.}}$  are based on the observed absolute B-band (Table 1) and the calculated B-H color using eq. 16.

We now estimate the error of the calculated stellar mass due to different galaxy evolution models and theoretical stellar-mass-to-light ratios. Consider one galaxy with observed blue-band luminosity,  $L_B$ , and current star formation rate,  $SFR$ . Two different theoretical stellar-mass-to-light ratios,  $\Upsilon_1$  and  $\Upsilon_2$ , lead to two different stellar masses,  $M_{*,1}$  and  $M_{*,2}$ . The logarithmic difference of the two corresponding stellar mass buildup times,  $\tau_{*,1}$  and  $\tau_{*,2}$ , is

$$\begin{aligned} \log \tau_{*,2} - \log \tau_{*,1} &= \log \frac{\tau_{*,2}}{\tau_{*,1}} = \log \frac{M_{*,2} SFR}{SFR M_{*,1}} \\ &= \log \frac{M_{*,2} SFR L_B}{L_B SFR M_{*,1}} = \log \frac{\Upsilon_2}{\Upsilon_1} \\ &= \log \Upsilon_2 - \log \Upsilon_1 . \end{aligned} \quad (18)$$

Note that  $L_B$  and  $SFR$  can be crossed out, because they refer to the same galaxy.

In Fig. 9 the stellar-mass-to-light ratio is plotted as a function of the total blue-band magnitude for the different galaxy evolution models listed in Tab. 3. For the least massive galaxies the model variation in the stellar-mass-to light ratio is about  $\pm 0.05$  dex around the mean value relation and becomes smaller for more massive galaxies. Therefore, for the purpose of this analysis the uncertainty in the calculation of the current stellar mass due to galaxy evolution can be neglected.

For the case of a constant galaxy-wide IMF the resulting stellar-mass buildup times as a function of the total stellar mass are plotted in Fig. 10. The average value of the stellar-mass buildup time is constant for galaxies more massive than  $10^8 M_\odot$  and increases by more than one order of magnitude for less massive ones. This implies that the SFR in massive galaxies has decreased much more slowly over cosmic time than for the least massive galaxies. This is in contradiction to the finding of downsizing, according to which massive disk galaxies have on average older stellar populations than dwarf galaxies.

When using  $H\alpha$  as a SFR tracer, in the IGIMF context the SFRs are much higher than the constant IMF-based SFRs for low SFR galaxies, i.e. less massive galaxies. The corresponding stellar-mass buildup times therefore become shorter. Indeed, for both IGIMF models, standard (Fig. 11) and minimum (Fig. 12), the stellar-mass buildup times decrease monotonically with decreasing

galaxy stellar mass. This suggests that massive disk galaxies have been forming stars at about a constant rate for a Hubble time, while dwarf galaxies have either turned on more recently or have a slightly increasing SFH, in full agreement with downsizing.

## 7. Conclusion

We have applied the revised  $SFR-L_{H\alpha}$  relation, which takes the nature of clustered star formation into account, to a significantly larger sample of star forming galaxies of the local volume than was available in Pflamm-Altenburg et al. (2007).

The SFRs of galaxies and the corresponding gas depletion and stellar-mass buildup time scales are calculated. Comparing these new values with the classical ones which are derived from SFRs based on an assumed constant galaxy-wide IMF, the changes are dramatic:

The SFRs of galaxies scale linearly with the total galaxy neutral gas mass and the corresponding gas depletion time scales are independent of the galaxy neutral gas mass. This implies that dwarf galaxies have the same star formation efficiencies as large disk galaxies. Furthermore, the stellar-mass buildup times are only compatible with downsizing in the IGIMF context. They are inconsistent with downsizing in the classical theory which assumes an invariant galaxy-wide IMF.

These results follow from the  $SFR_{H\alpha}/SFR_{FUV}$  data compiled by Lee et al. (2009), independently of the well developed IGIMF theory. The IGIMF theory merely explains the Lee et al. (2009) results within an empirically well established star-formation framework. The success of the IGIMF theory, developed by Kroupa & Weidner (2003) and Weidner & Kroupa (2005, 2006), is that the Lee et al. (2009) results have been predicted (Pflamm-Altenburg et al. 2007) rather than being adjusted afterwards. The power of the IGIMF theory lies in that it is readily computable and deterministic.

We emphasise that the galaxy properties derived in the IGIMF theory are qualitatively independent of the main parameter of the IGIMF, the slope of the ECMF. For the full range of possible slopes of the ECMF in the IGIMF theory SFRs of dwarf galaxies are significantly higher than derived in the classical paradigm assuming a con-

stant galaxy-wide IMF independent of the global SFR.

The revision of the SFRs of dwarf galaxies suggested here now poses a major challenge for our theoretical understanding of star formation in galaxies which had been developed with the aim of explaining the low star formation efficiencies of dwarf galaxies. It follows that galaxy and cosmic evolution models need a substantial revision requiring further studies.

## REFERENCES

- Bastian, N. 2008, MNRAS, 390, 759
- Bell, E. F. & de Jong, R. S. 2001, ApJ, 550, 212
- Bothwell, M. S., Kennicutt, R. C., & Lee, J. C. 2009, MNRAS - in press
- Chabrier, G. 2003, PASP, 115, 763
- Cole, S., Lacey, C. G., Baugh, C. M., & Frenk, C. S. 2000, MNRAS, 319, 168
- Corbelli, E. & Schneider, S. E. 1997, ApJ, 479, 244
- Dame, T. M., Koper, E., Israel, F. P., & Thaddeus, P. 1993, ApJ, 418, 730
- Diehl, R., Halloin, H., Kretschmer, K., et al. 2006, Nature, 439, 45
- Elmegreen, B. G. 1997, ApJ, 486, 944
- Elmegreen, B. G. 1999, ApJ, 515, 323
- Gallagher, III, J. S., Hunter, D. A., & Tutukov, A. V. 1984, ApJ, 284, 544
- Hindman, J. V. 1967, Australian Journal of Physics, 20, 147
- Hoversten, E. A. & Glazebrook, K. 2008, ApJ, 675, 163
- Kaisin, S. S. & Karachentsev, I. D. 2008, A&A, 479, 603
- Karachentsev, I. D. & Kaisin, S. S. 2007, AJ, 133, 1883
- Karachentsev, I. D., Karachentseva, V. E., Huchtmeier, W. K., & Makarov, D. I. 2004, AJ, 127, 2031
- Kennicutt, Jr., R. C. 1983, ApJ, 272, 54
- Kennicutt, Jr., R. C. 1998a, ARA&A, 36, 189
- Kennicutt, Jr., R. C. 1998b, ApJ, 498, 541
- Kennicutt, Jr., R. C., Bresolin, F., Bomans, D. J., Bothun, G. D., & Thompson, I. B. 1995, AJ, 109, 594
- Kennicutt, Jr., R. C., Calzetti, D., Walter, F., et al. 2007, ApJ, 671, 333
- Kennicutt, Jr., R. C., Tamblyn, P., & Congdon, C. E. 1994, ApJ, 435, 22
- Kirby, E. M., Jerjen, H., Ryder, S. D., & Driver, S. P. 2008, AJ, 136, 1866
- Köppen, J., Weidner, C., & Kroupa, P. 2007, MNRAS, 375, 673
- Kroupa, P. 2001, MNRAS, 322, 231
- Kroupa, P. 2002, Science, 295, 82
- Kroupa, P. & Weidner, C. 2003, ApJ, 598, 1076
- Kunth, D. & Sargent, W. L. W. 1986, ApJ, 300, 496
- Lada, C. J. & Lada, E. A. 2003, ARA&A, 41, 57
- Larsen, S. S. 2009, A&A, 494, 539
- Lee, J. C., Gil de Paz, A., Tremonti, C., et al. 2009, ApJ - in press
- Legrand, F., Tenorio-Tagle, G., Silich, S., Kunth, D., & Cerviño, M. 2001, ApJ, 560, 630
- Löckmann, U., Baumgardt, H., & Kroupa, P. 2009, submitted
- Mateo, M. L. 1998, ARA&A, 36, 435
- Meurer, G. R., Wong, O. I., Kim, J. H., et al. 2009, ApJ, 695, 765
- Miller, G. E. & Scalo, J. M. 1979, ApJS, 41, 513
- Pflamm-Altenburg, J. & Kroupa, P. 2008, Nature, 455, 641
- Pflamm-Altenburg, J., Weidner, C., & Kroupa, P. 2007, ApJ, 671, 1550
- Pflamm-Altenburg, J., Weidner, C., & Kroupa, P. 2009, MNRAS, 395, 394



- Recchi, S., Calura, F., & Kroupa, P. 2009, *A&A*, 499, 711
- Skillman, E. D., Côté, S., & Miller, B. W. 2003, *AJ*, 125, 593
- van den Bergh, S. 1999, *A&A Rev.*, 9, 273
- van Zee, L. 2001, *AJ*, 121, 2003
- Verley, S., Hunt, L. K., Corbelli, E., & Giovanardi, C. 2007, *A&A*, 476, 1161
- Walterbos, R. A. M. & Braun, R. 1994, *ApJ*, 431, 156
- Weidner, C. & Kroupa, P. 2005, *ApJ*, 625, 754
- Weidner, C. & Kroupa, P. 2006, *MNRAS*, 365, 1333
- Weidner, C., Kroupa, P., & Bonnell, I. 2009, *MNRAS* – in press
- Weidner, C., Kroupa, P., & Larsen, S. S. 2004, *MNRAS*, 350, 1503
- Westerlund, B. E. 1997, *Cambridge Astrophysics Series*, 29

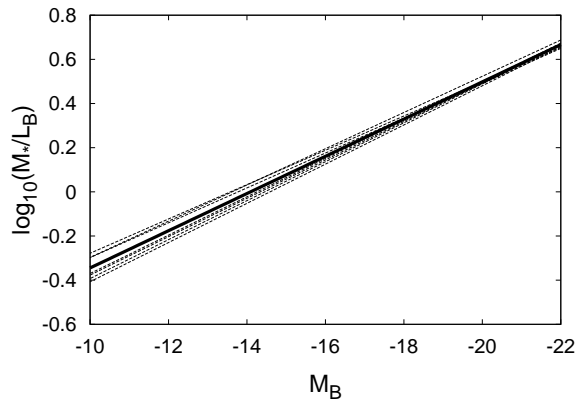


Fig. 9.— The stellar-mass-to-light ratio as a function of the blue-band magnitude resulting from combining eq. 16 and 13 with Tab. 3. Each dotted line represents one individual galaxy evolution model and the solid line shows the mean value relation. Note that the increase of  $M_*/L_B$  with  $M_B$  is not a result of the IGIMF effect but occurs as a result of using the empirical relation (eq. 16) in the constant-IMF modelling of Bell & de Jong (2001).

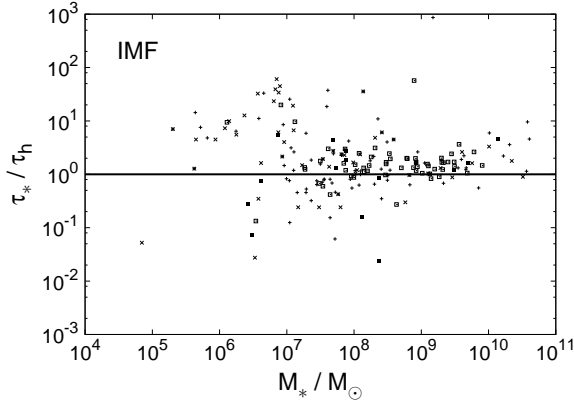


Fig. 10.— The stellar mass buildup time scale in units of the Hubble time,  $\tau_h = 13.7$  Gyr, in dependence of the total stellar mass derived from the blue luminosity for a constant galaxy-wide IMF. Note that the buildup times for dwarf star forming galaxies are longer than the ones for large disk galaxies. This implies that the SFRs of dwarf galaxies must have decreased faster over cosmic time than the SFRs of large disk galaxies. This is in contradiction to the finding of downsizing according to which the SFRs of large disk galaxies must have decreased faster over cosmic time than the SFRs of dwarf galaxies. The symbols are the same as in Fig. 2.

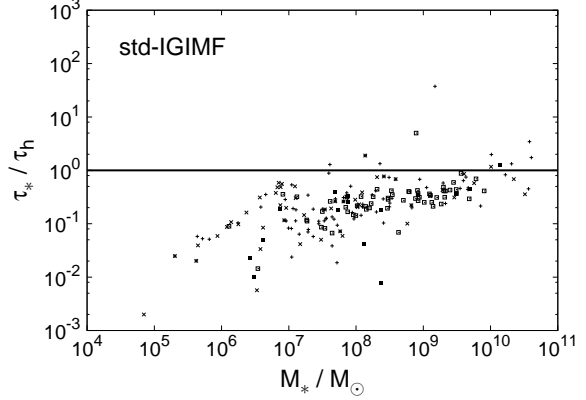


Fig. 11.— The same as Fig. 10 but for the standard IGIMF. Note that the stellar mass buildup times, which result from SFR calculations in the IGIMF context, decrease with decreasing galaxy mass. This suggests that the SFR may have been increasing slightly with time for dwarf galaxies or that they were forming stars over a more recent epoch while for massive disk galaxies the SFHs may be constant, which is in agreement with downsizing. The symbols are the same as in Fig. 2.

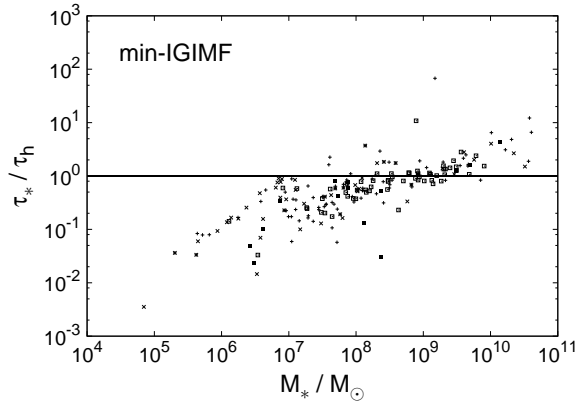


Fig. 12.— The same as Fig. 11 but for the minimum IGIMF. The symbols are the same as in Fig. 2.